Study of Nitrate Stress in *Desulfovibrio vulgaris* Hildenborough Using iTRAQ Proteomics

A. M. Redding, A. Mukhopadhyay, D. Joyner, T. C. Hazen, J. D. Keasling

University of California, Berkeley; Lawrence Berkeley National Laboratory

DISCLAIMER

Study of Nitrate Stress in *Desulfovibrio vulgaris* Hildenborough Using iTRAQ Proteomics

A. M. Redding, A. Mukhopadhyay, D. Joyner, T. C. Hazen, J. D. Keasling

Abstract

The response of *Desulfovibrio vulgaris* Hildenborough (*Dv*H), a sulfate-reducing bacterium, to nitrate stress was examined using quantitative proteomic analysis. *Dv*H was stressed with 105 mM $NaNO_3$, a level that caused a 50% inhibition in growth. The protein profile of stressed cells was compared to that of cells grown in the absence of nitrate using the iTRAQ peptide labeling strategy and tandem liquid-chromatography separation coupled to mass spectrometry (quadrupole time-of-flight) detection. A total of 737 unique proteins were identified by two or more peptides, representing 22% of the total *Dv*H proteome and spanning every functional category. The results indicate that this was a mild stress, as proteins involved in central metabolism and the sulfate reduction pathway were unperturbed. Proteins involved in the nitrate reduction pathway increased. Increases seen in transport systems for proline, glycine-betaine and glutamate indicate that the $NaNO_3$ exposure led to both salt stress and nitrate stress. Up-regulation observed in oxidative stress response proteins (Rbr, RbO, etc.) and a large number of ABC transport systems as well as in iron-sulfur cluster containing proteins, however, appear to be specific to nitrate exposure. Finally, a number of hypothetical proteins were among the most significant changers, indicating that there may be unknown mechanisms initiated upon nitrate stress in *Dv*H.

Introduction

Anaerobic sulfate-reducing bacteria (SRB) such as *Desulfovibrio vulgaris* Hildenborough (*Dv*H) play an important role in global sulfur cycling [1]. The *Desulfovibrio* genus has long been implicated in bio-corrosion and souring of petroleum [2-4], making it an important research organism. Reports that the c_3 cytochrome of *Dv*H is capable of reducing uranium and chromate [5, 6] have made it a promising candidate for bio- and geo-remediation efforts, which in turn provide compelling reasons to study the physiology of this organism. Contaminated sites present a very complex biological environment to bacteria, including not only toxic and excess metal ions, but also other contaminants such as high concentrations of salt, low pH, and high levels (> 500 mM) of nitrate [7]. The presence of alternate electron acceptors, such as nitrate, can significantly alter the physiology of bacteria, and consequently impact bioremediation. This study investigated the changes initiated in the *Dv*H proteome in response to perturbation by the addition of sodium nitrate.

Protein staining coupled with 2D-PAGE has been the most widely used method to quantify proteins prior to identification with mass spectrometry [8]. However, hydrophobic proteins are difficult to separate on 2D gels, and quantification of proteins becomes limited by the sensitivity of the protein stain used [8, 9]. Peptide tagging strategies are more sensitive methods to survey proteins, as their sensitivity is limited at the level of mass spectrometry, rather than protein staining [10]. Additionally, the use of liquid chromatography to resolve proteolyzed proteomes enables higher throughput compared to gel-based strategies. Early peptide tagging techniques, such as ICAT labeling, limited the number of observable proteins by only addressing cysteine-containing peptides, and only allowed comparison of two different conditions [11, 12]. Further, an ICAT sample contains peptides represented by two unique masses (heavy and light).

In contrast, the iTRAQ technique uses isobaric tags to differentially label proteins from up to 4 different conditions and compares them simultaneously [13]. iTRAQ tags label N-terminal amines and lysine residues, essentially labeling every peptide in the mixture. Being isobaric, no additional complexity is introduced in the mass spectra collected, as each peptide sequence elutes at one time and at the same mass. However, because the entire proteome is present for analysis, more extensive resolution is required to obtain high quality, reproducible data. This study describes the optimization of proteomic methods to study a nitrate perturbation in *Dv*H using the iTRAQ technique.

Material and Methods

Culture Maintenance. *Desulfovibrio vulgaris* Hildenborough, ATCC 29579 (Manassas, VA), was grown in lactate-sulfate version 4 medium (LS4D). LS4D is a defined medium for culturing sulfate reducers and is based on Postgate medium [14]. LS4D consists of 50 mM $NaSO_4$, 60 mM sodium lactate, 8 mM $MgCl_2$, 20 mM NH_4Cl, 2.2 mM KH_2PO_4, 0.6 mM $CaCl_2$, 30 mM PIPES buffer, 0.064 μM resazurin, 10 mM NaOH, 1 ml/L Thauers vitamins [15], 12.5 ml/L trace minerals, and 5ml/L titanium citrate. The trace mineral stock contains 50 mM nitrilotriacetic acid, 5 mM $FeCl_2$•$4H_2O$, 2.5 mM $MnCl_2$•$4H_2O$, 1.3 mM $CoCl_2$•$6H_2O$, 1.5 mM $ZnCl_2$, 210 μM Na_2MoO_4•$4H_2O$, 320 μM H_3BO_3, 380 μM $NiSO_4$•$6H_2O$, 10 μM $CuCl_2$•$2H_2O$, 30 μM Na_2SeO_3, and 20 μM Na_2WO_4•$2H_2O$. *Dv*H cultures from ATCC were grown to mid log phase in 1 L of LS4D, checked for purity, dispensed into 2 mL cryogenic vials (Nalgene) with 0.5 ml 30% glycerol, and frozen at -80°C until used. To minimize phenotypic drift from repetitive culturing, all experiments were started from frozen stocks and were performed using cells less than three subcultures from the original ATCC culture. All incubations were done at

30°C. Under these conditions, *Dv*H generation time was 5 h with a mid-log phase density of 3×10^8 cells/mL (OD_{600} of 0.3). The final yield density was approximately 3×10^9 (OD_{600} of 0.7). All experiments, inoculations, and transfers were done in an anaerobic glove chamber (Coy Laboratory Products Inc., Grass Lake, MI) with an atmosphere of 5% CO_2, 5% H_2 and 90% N_2.

Minimum Inhibitory Concentrations. The minimum inhibitory concentration (MIC) was defined as the concentration of a stressor that caused a doubling in the generation time and/or decreased the overall yield by 50% without causing significant cell death. To determine MICs for *Dv*H, growth curves were performed in a 96-well plate. Each well was inoculated with 10% mid-log phase *Dv*H cells with six replicates of each stressor dilution. The 96-well plates were placed in airtight Retain bags (Nasco, Modesto, CA) and thermal sealed while under an anaerobic atmosphere. Sealed plates were placed in the OmniLog® instrument (Biolog Inc., Hayward, CA) where readings were taken every 15 min for 150 h. The OmniLog® instrument was calibrated against *Dv*H cell densities as measured by a spectrophotometer at OD_{600}, a Biolog plate reader OD_{590}, and direct cell counts. All were comparable at 95% confidence interval for exponential growth phase. A kinetic plot of the *Dv*H growth was used to determine generation time and cell yield.

Biomass Production. Frozen stocks were used as a 10% inoculum in 100 mL of LS4D (starter culture). This starter culture was allowed to grow until it reached mid-log phase growth and was verified for purity by microscopy and spread plates (anaerobic and aerobic). Two-liter production cultures were inoculated with 10% starter culture. All production cultures were grown in triplicate (three control cultures and three stressed cultures). When the production cultures reached an OD_{600} of 0.3, 50 mL of sample were taken from each culture and pooled (300 mL total volume) as T0. Once sampling was completed, degassed $NaNO_3$ solution was added to

the three stressed cultures to a final concentration of 105 mM, and an equivalent volume of sterile distilled, degassed water was added to each control culture. Six-hundred (600) mL of sample (100 mL each from the 3 control cultures and 100 mL each from the 3 stressed cultures) were collected at 480 min post-exposure, while cells were still in exponential growth phase. To minimize sample variability due to processing time, samples were pulled by peristaltic pump through 7 m of capillary tubing submerged in an ice bath, which dropped the sample temperature to 4°C in less than 15 sec. The chilled samples were centrifuged at 6,000 × g for 10 min at 4°C, the pellet was washed with 4°C, degassed, sterile, phosphate-buffered saline and centrifuged again at 6,000 × g for 10 min at 4°C. Supernatant was discarded, and the final pellet was flash frozen in liquid nitrogen and stored at -80°C until analyzed.

Sample Preparation and Labeling. Cell pellets were resuspended in 1 mL of 500 mM triethylammonium bicarbonate buffer (TEAB, Sigma). Cell suspensions on ice were sonicated using a sonicator (VirSonic, Gardiner, NY) equipped with a micro tip for a total of 3 minutes with pulses (5 sec on, 10 off). Lysed cells were clarified by centrifugation for 30 minutes at 20817 × g. The clarified supernatant was used as total cellular protein. The BCA protein assay (Pierce) was used to determine final protein concentration of each sample. One-hundred fifty (150) micrograms of protein was taken from each sample and was denatured, reduced, blocked, digested, and labeled with isobaric reagents as per manufacturer's directions (Applied Biosystems), with 3 vials of reagent used per sample. The samples were labeled as follows: tag_{114}, T0 control; tag_{115}, 480 min control; tag_{116}, 480 min nitrate; and tag_{117}, 480 min nitrate. Tag_{116} and tag_{117} provided a technical replicate to allow assessment of internal error.

Strong Cation Exchange Fractionation. Strong cation exchange (SCX) fractionation was completed using an Ultimate HPLC with Famos Micro Autosampler and UV detector

(Dionex-LC Packings, Sunnyvale, CA, USA). Labeled samples were pooled and diluted 10 fold with buffer A (25% ACN, 0.1% formic acid) to reduce salt concentration. The pH of the sample was adjusted to 3.0 with formic acid (FA) before being loaded onto a PolyLC Polysulfoethyl A column (4.6 mm × 100 mm). Buffer B was composed of 800 mM KCl, 25% ACN, and 0.1% FA. Sample fractionation was completed using a three step gradient, as follows: 0-15% B in 15 min, 15-30% B in 30 min, and 30-100% B in 13 min. Forty-four fractions were collected at a flow rate of 700 μl/min on the basis of the UV trace at 214 nm. Several fractions were pooled post-collection to yield a total of 21 sample containing fractions.

Reverse-Phase Separation and Mass Spectrometry. Fractions were partially evaporated to remove ACN and desalted using C18 MacroSpin Columns (Nest Group, Southborough, MA) according to manufacturer's directions. Desalted fractions were dried using a vacuum centrifuge and reconstituted in 86 μL 0.1% FA. In each run, 40 μL of each sample were auto-injected using an Ultimate HPLC with Famos Autosampler and Switchos Micro Column Switching Module (Dionex-LC Packings, Sunnyvale, CA) onto a PepMap100 trapping column (0.3 mm × 5 mm). Reverse-phase separation was completed on a PepMap 100 column (75 μm × 15 cm) at a flow rate of 200 nL/min using buffers 2% ACN, 0.1% FA (A) and 80% ACN, 0.1% FA (B). The gradient was run as follows: 0-30% B in 120 min, 30-100% B in 5 minutes, 100% B for 10 minutes, 100-0% B in 5 minutes, and 0% B for 20 minutes. The samples were directly injected into an ESI-QTOF Mass Analyzer (QSTAR® Hybrid Quadrupole TOF, Applied Biosystems, Framingham, MA) using electrospray ionization. Two product ion scans were set to be collected for each cycle. Ions had to exceed a threshold of 50 counts to be selected as parent ions for fragmentation. Parent ions and their isotopes were excluded from further selection for one minute. A mass tolerance of 100 ppm was designated. The instrument was manually calibrated

and tuned following each batch of two to four samples. BSA was used as a standard to evaluate system performance, and was run at least once per day during sample analysis to verify separation, identification, peak shape and mass accuracy.

MS Analysis and Protein Identification. Collected mass spectrograms were analyzed using Analyst 1.1 with ProID 1.1, ProQuant 1.1, and ProGroup 1.0.6 (Applied Biosystems). Protein identifications were confirmed using MASCOT version 2.1. A FASTA file containing all the ORF protein sequences of *Dv*H, obtained from microbesonline.org [16], was used to form the theoretical search database. The same parameters were used in both programs; namely, trypsin was the cleavage enzyme, and mass tolerances of 0.1 for MS and 0.15 for MS/MS were used. Peptides with charges from +2 to +4 were searched. In ProQuant, 5 matches were saved per protein and all peptides above a confidence of 2 were stored. All matches above a 95% confidence interval were considered. Scripts were written using Python to collate data between Run 1 and Run 2 and between MASCOT and ProGroup. Only proteins identified by at least two unique peptides by ProQuant and MASCOT were considered for further analysis.

Quantification of Relative Change. All protein ratios were obtained from the ProQuant database using ProGroup. Tag ratios for each protein are a weighted average from peptides of all confidence that are uniquely assigned to that protein. Because tag_{116} and tag_{117} were technical replicates, the reported ratios are the average of $\log_2(116/115)$ and $\log_2(117/115)$. The internal error was defined as the value at which 95% of all proteins had no deviation from each other, where the deviation was the absolute value of the difference between $\log_2(116/115)$ and $\log_2(117/115)$. The internal errors were 0.12 (Run 1) and 0.2 (Run 2). The deviation between Run 1 and Run 2 was the absolute value of the difference between $\log_2(116/115)$. Ninety percent

(90%) of all proteins fell within a deviation of 0.4. Proteins with quantitation data from both runs and having ratios exceeding 0.4 were considered significant changers.

Results and Discussion

When applying a perturbation to a cellular system, it becomes critical to ensure that the majority of the population remains alive. The minimum inhibitory concentration (MIC) of sodium nitrate was determined to be 105 mM in *Dv*H grown in LS4D medium. Using the MIC as a guide ensures that the culture has experienced an environmental change as measured by a reduction in cell growth. The viability of cultures was confirmed using microscopy and plating to minimize artifacts due to cell death.

Cell pellets were lysed and processed as described to produce a proteolyzed pool of peptides, which were resolved using a SCX column. Two replicate analyses of the 21 SCX fractions were completed, generating a total of 25,607 spectra. The data collected from these samples were analyzed both using ProQuant (Applied Biosystems) and MASCOT. Using ProQuant analysis, a total of 1,166 proteins were uniquely identified between the two runs at a 95% confidence interval (CI) from a total of 5,683 unique, high confidence peptides. Mascot identified a total of 1,221 proteins above 95% confidence interval. A total of 1,047 proteins were identified commonly between the two data sets. Utilizing an algorithm to assign spectra to peptides, even under stringent conditions, does leave the possibility for incorrect assignment. Therefore, only proteins identified on the basis of at least two unique and high confidence peptides and identified by both software packages were considered, resulting in identification of 737 proteins. Interestingly, several proteins that were identified by at least two unique peptides in ProQuant were not identified by Mascot, and visa versa. More information regarding the

underlying computational algorithms used for peptide identification would be required to explain these differences. In absence of such information, these proteins were excluded from further analysis. *Dv*H has been annotated to have 3,396 protein-coding open reading frames; however, several of these proteins may not include tryptic digestion sites or may generate peptides outside of the mass range (800-3000 Da) for mass spectrometry. Without excluding any proteins, 22% of the total proteome was observed in this study. During annotation, functional assignment for each protein was made using the nomenclature developed for clusters of orthologous groups (COGs). All identified proteins were grouped by COG category; every functional category was represented.

Duplicate labeling of the nitrate stressed sample provided a direct technical replicate for the ratios obtained in each run. Ideally, the ratio of these two tags to each other should equal one. The internal error for each run was computed as described above. The first run had an overall internal error of 0.12, and the second had an error of 0.2. One-hundred eighty-six proteins had a ratio that exceeded the internal error in both runs and were considered to be potentially changing. The two separate runs were also technical replicates of one another, which allowed a calculation of the error between the two runs. The error between two separate analyses was 0.4, which was significantly greater than the internal error of either run alone (Figure 1a). Sixty-five proteins had ratios exceeding 0.4 in all runs, and are therefore considered to be the most significant changers (Figure 1b). Tables of all observed proteins are available in the supplementary material.

*Dv*H has been annotated to have a nitrate reductase, DsrM, for converting nitrate to nitrite, which is the first step in assimilatory nitrate reduction. The nitrite reductase NrfA is present and has been demonstrated to convert nitrite to ammonia [17]. From ammonia there are

many pathways to incorporate nitrate into biomass (Figure 2). The proteomics data included proteins for many of the steps in this pathway (Table 1). The levels of several of the proteins increased, suggesting an increased flux through this pathway. However, it is important to note that many proteins do not require up- or down-regulation to change flux through a pathway; therefore, flux measurements must be determined independently. The one notable protein not observed in this pathway was the nitrate reductase, DsrM. It was postulated that DsrM may be inactive, since previous experiments have shown that nitrate was not measurably reduced at levels of 10 mM, while sulfate was reduced [17].

Upon perturbation by nitrate, the cellular growth rate decreased by half. Consequently, it was anticipated that the proteome of the stressed cells would indicate the mechanism for the inhibitory role of nitrate. However, there are few significant changes in the proteome that address this issue. Several thioredoxin reductase proteins (DVU0283, DVU1457, and DVU2247) were mildly down-regulated, while DVU3379, which oxidizes thioredoxin, was mildly up-regulated (Table 2). Thioredoxins are housekeeping enzymes involved in maintaining cellular energy levels, so changes in these proteins may be reflective of the decrease in growth rate. Several oxidative stress proteins, including SodB, Rbr2 and RbO, increased significantly during nitrate stress. Additionally, the levels of nigerythrin and a thiol peroxidase, both involved in superoxide removal, increased. These are signature proteins of the SRB class of bacteria, and may be involved in global stress response. A regulon involving many oxidative response genes, known as the PerR regulon, has been predicted in *Dv*H [18]. As can be seen, the members of this predicted regulon do not change similarly at the proteomic level (Table 2). Several chemotaxis proteins increased, although flagellin decreased. The levels of the periplasmic binding domains of 13 ABC transporters, seven of which transport amino acids, increased. ABC transporters

form the largest annotated group of significantly changing proteins. Eleven of the most significantly changing proteins are hypothetical proteins with no known homologs, indicating that the mechanism of nitrate response in *Dv*H is different from that in other studied bacteria. Additionally, the levels of several response regulators increased, which provides a foundation for more focused studies (Table 3).

Sodium, which was added in equimolar concentration to the nitrate, is a co-stressor in these experiments. Consequently, osmoprotection mechanisms employed to cope with osmotic stress may be expected to change. The level of the glycine/betaine/l-proline transporter, DVU2297, increased in response to salt stress during the nitrate perturbation, as both proline and betaine are well documented osmoprotectants [19-21]. Down-regulation of DVU1953 and DVU0161, both of which convert glutamate to glutamine, was observed. Both glutamate and glutamine are documented to be osmoprotectants [22]; however, an increase in proteins that convert glutamine to glutamate was not detected (Figure 2). This indicates that *Dv*H may utilize glutamate in preference to glutamine in osmoprotection. Taken together, these data suggest that the mechanisms to counter osmotic stress in *Dv*H are very sensitive to changes in the osmolarity of the medium.

Nitrate serves as an alternate electron acceptor for many anaerobic sulfate-reducing bacteria [23]. Although *Dv*H has never been shown to grow on nitrate, it is possible that the presence of additional electron acceptors could inhibit the sulfate reduction pathway. Both the assimilatory and dissimilatory sulfite reductases, DVU1597 and DVU0404, respectively, increased. However, there were no observable changes in other parts of the sulfate reduction pathway (Table 4). Computational studies have been done to locate a regulon containing the genes for sulfate-reduction [18], a primary source of energy for SRB. The HcpR regulon was

identified as a potential candidate because several key sulfate-reducing proteins form part of the regulon (Table 3). One of the key members of the regulon is a hybrid cluster protein (HCP), DVU2543, previously known as the prismane protein [24, 25]. In other organisms, orthologs of this gene have been shown to respond to nitrate and nitrite [26-28], and microarray data in *Dv*H have shown that it increases significantly in the presence of nitrite [18]. Increased levels of this protein, in addition to CooX, and CooU, were noted, while the levels of other proteins involved in this regulon did not change. In addition to iron-sulfur cluster proteins, cytochromes also play a large role in channeling electrons through the cell. Cytochrome c-553 increased, along with HemC, which is involved in heme biosynthesis.

Other groups have examined gene expression in a *Dv*H mutant lacking *nrf*A [17], which is involved in nitrite reduction. In that study, down-regulation of the genes involved in the sulfate reduction pathway (*Dsr*AB), electron transport complexes (*qmo*ABC and *dsr*MKJOP), and the ATP synthase were observed. In this study, the levels of these proteins did not change (Table 4). This may indicate that these pathways are only responsive to high nitrite concentrations, that the protein levels are insensitive to changes in transcript levels, or that these pathways only respond to the deletion of *nrfA*.

Conclusions

Using quantitative peptide tagging and a rigorous peptide resolution technique, a large proteomics data set was generated for studying the results of nitrate perturbation in the sulfate reducing bacterium *Dv*H. Data curation plays an important first step in determining which proteins are present in a sample. Unlike microarray analysis, there is not yet a standard data analysis protocol for proteomics. In an attempt to eliminate dubious proteins, data were

combined from both ProGroup and MASCOT. Only proteins with at least two unique, high-confidence peptides sequenced by both software packages were considered. While this significantly reduced the size of the final data set, there were enough differences between the results from both ProGroup and MASCOT so as to raise questions about the absolute accuracy of either by itself. Following these criteria, 737 proteins were considered to be identified in this study. The use of ProGroup was required to obtain quantitative ratios. The use of internal replicates and duplicate runs allowed us to determine meaningful changes. One-hundred eighty-five proteins changed above the level of internal error in all runs and were considered potentially changing. The ratios of sixty-five of those proteins exceeded the error between replicate analyses, and were therefore considered as significantly changing. These proteins were examined to find changes due to nitrate stress.

It was expected that, while nitrate by itself may not prove harmful, the use of nitrate as an electron acceptor would generate the harmful intermediate nitrite, causing nitrite stress to be observed in the proteome. While growth is hampered in the presence of 105 mM nitrate, most central pathways and cellular machinery remain unperturbed. Nitrate-related changes were observed in the nitrate-to-ammonia conversion pathway. As this study addressed the immediate response of the bacterium to the presence of nitrate, both proteins changing in quantities as well as those that are present in levels equal to those in the control cells may play important roles in cellular response to stress. The presence of a large number of hypothetical proteins among the most significantly changing proteins after nitrate treatment indicates that important components of the nitrate response in *Dv*H utilize unknown mechanisms. ABC transport proteins made up the largest group of known proteins that changed in response to this treatment; however further experiments are required to assign their change specifically to nitrate stress rather than a

hyperionic or sodium stress. The addition of 105 mM sodium nitrate clearly caused hyperionic stress and led to upregulation in proteins, such as DVU2297, most certainly involved in countering an osmotic stress. Global responses included signature proteins such as Rbr2, Rbo, and SodB. Using *Dv*H as a model organism, the changes in characteristic SRB proteins under a variety of conditions will allow development of models for global response mechanisms in SRB.

Acknowledgements

This work was part of the Virtual Institute for Microbial Stress and Survival (http://vimss.lbl.gov) supported by the U. S. Department of Energy, Office of Science, Office of Biological and Environmental Research, Genomics:GTL Program through contract DE-AC02-05CH11231 with LBNL. We acknowledge Applied Biosystems for providing the ProGroup patch to facilitate data analysis. The authors would like to thank Chris Petzold for useful discussions and support.

References

1. Gest H. Biochemistry and Physiology of Anererobic bacteria, ed. L. Ljundgdahl, G., Adams, Michael, W., Barton Larry, L., Ferry, James, G., Johnson, Michael, K. New York: Springer-Verlag, 2003.
2. Hadas O, Pinkas R. Sulfate Reduction Processes in Sediments at Different Sites in Lake Kinneret, Israel. Microbial Ecology, 1995; 30:55-66.
3. Tabak HH, Govind R. Advances in biotreatment of acid mine drainage and biorecovery of metals: 2. Membrane bioreactor system for sulfate reduction. Biodegradation . 2003; 14:437-452.
4. Benbouzidrollet ND, Conte M, Guezennec J, et al. Monitoring of a vibrio-natriegens and desulfovibrio-vulgaris marine aerobic biofilm on a stainless-steel surface in a laboratory tubular flow system. Journal of Applied Bacteriology, 1991; 71:244-251.
5. Lovley DR, Widman PK, Woodward JC, et al. Reduction of Uranium by Cytochrome-C(3) of Desulfovibrio-Vulgaris. Applied and Environmental Microbiology, 1993; 59(11):3572-3576.
6. Lovley DR, Phillips EJP. Reduction of Chromate by Desulfovibrio-Vulgaris and Its C(3) Cytochrome. Applied and Environmental Microbiology, 1994; 60(2):726-728.
7. NABIR Field Research Center. http://www.esd.ornl.gov/nabirfrc/index.html. (January 2006, date last accessed).
8. Righetti PG, Campostrini N, Pascali J, et al. Quantitative proteomics: a review of different methodologies. Eur J Mass Spectrom, 2004; 10(3):335-348.
9. Choe LH, Aggarwal K, Franck Z, et al. A comparison of the consistency of proteome quantitation using two-dimensional electrophoresis and shotgun isobaric tagging in Escherichia coli cells. Electrophoresis, 2005; 26(12):2437-49.
10. Putz S, Reinders J, Reinders Y, et al. Mass spectrometry-based peptide quantification: applications and limitations. Expert Rev Proteomics, 2005; 2(3):381-92.
11. Li J, Steen H, Gygi SP. Protein Profiling with Cleavable Isotope-coded Affinity Tag (cICAT) Reagents: The Yeast Salinity Stress Response. Mol Cell Proteomics, 2003; 2(11):1198-204.
12. Smolka MB, Zhou H, Purkayastha S, et al. Optimization of the isotope-coded affinity tag-labeling procedure for quantitative proteome analysis. Anal Biochem, 2001; 297(1):25-31.
13. Ross PL, Huang YN, Marchese JN, et al. Multiplexed protein quantitation in Saccharomyces cerevisiae using amine-reactive isobaric tagging reagents. Mol Cell Proteomics, 2004; 3(12):1154-69.
14. Postgate JR, The Sulfate-Reducing Bacteria. Cambridge: Cambridge University Press, 1984.
15. Brandis A, Thauer RK. Growth of Desulfovibrio Species on Hydrogen and Sulfate as Sole Energy-Source. Journal of General Microbiology, 1981; 126(SEP):249-252.
16. Alm EJ, Huang KH, Price MN, et al. The MicrobesOnline Web site for comparative genomics. Genome Res, 2005; 15(7):1015-22.
17. Haveman SA, Greene EA, Stilwell CP, et al. Physiological and gene expression analysis of inhibition of Desulfovibrio vulgaris hildenborough by nitrite. J Bacteriol, 2004; 186(23):7944-50.
18. Rodionov DA, Dubchak I, Arkin A, et al. Reconstruction of regulatory and metabolic pathways in metal-reducing delta-proteobacteria. Genome Biol, 2004; 5(11):R90.

19. Glaasker E, Tjan FS, Ter Steeg PF, et al. Physiological response of Lactobacillus plantarum to salt and nonelectrolyte stress. J Bacteriol, 1998; 180(17):4718-23.
20. Kappes RM, Kempf B, Kneip S, et al. Two evolutionarily closely related ABC transporters mediate the uptake of choline for synthesis of the osmoprotectant glycine betaine in Bacillus subtilis. Mol Microbiol, 1999; 32(1):203-16.
21. Ko R, Smith LT, Smith GM. Glycine betaine confers enhanced osmotolerance and cryotolerance on Listeria monocytogenes. J Bacteriol, 1994; 176(2):426-31.
22. Goude R, Renaud S, Bonnassie S, et al. Glutamine, glutamate, and alpha-glucosylglycerate are the major osmotic solutes accumulated by Erwinia chrysanthemi strain 3937. Appl Environ Microbiol, 2004; 70(11):6535-41.
23. Gibson GR. Physiology and ecology of the sulphate-reducing bacteria. J Appl Bacteriol, 1990; 69(6):769-97.
24. Cooper SJ, Garner CD, Hagen WR, et al. Hybrid-cluster protein (HCP) from Desulfovibrio vulgaris (Hildenborough) at 1.6 A resolution. Biochemistry, 2000; 39(49):15044-54.
25. Stokkermans JP, Pierik AJ, Wolbert RB, et al. The primary structure of a protein containing a putative [6Fe-6S] prismane cluster from Desulfovibrio vulgaris (Hildenborough). Eur J Biochem, 1992; 208(2):435-42.
26. Kim CC, Monack D, Falkow S. Modulation of virulence by two acidified nitrite-responsive loci of Salmonella enterica serovar Typhimurium. Infect Immun, 2003; 71(6):3196-205.
27. van den Berg WA, Hagen WR, van Dongen WM. The hybrid-cluster protein ('prismane protein') from Escherichia coli. Characterization of the hybrid-cluster protein, redox properties of the [2Fe-2S] and [4Fe-2S-2O] clusters and identification of an associated NADH oxidoreductase containing FAD and [2Fe-2S]. Eur J Biochem, 2000; 267(3):666-76.
28. Beliaev AS, Thompson DK, Khare T, et al. Gene and protein expression profiles of Shewanella oneidensis during anaerobic growth with different electron acceptors. Omics, 2002; 6(1):39-60.

Figure captions

Figure 1- Ratio comparisons. (a) Internal error is computed by plotting the ratios between tag116 and tag117 (circles). The error bars for the internal replicates are denoted (— - —). The amount of variation between tag116 in run 1 and tag116 in run 2 (technical replicates) is shown (triangles), along with the associated error (– – –). (b) The amount of sample variation between control and stressed samples (squares) are plotted along with the error bars from Fig.1a. There are 65 of proteins whose ratio between stressed and control exceed the amount of run to run variability, and are considered to be the significant changers.

Figure 2- Nitrate reduction pathway. The boxes show pathway intermediates, proteins involved in each function are listed below the arrows by name. Corresponding information about each protein can be found in Table 1.

Figures

Figure 1

a)

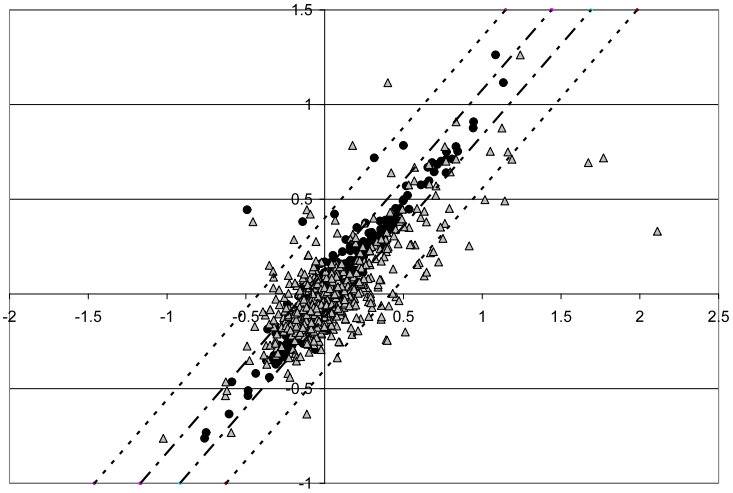

b)

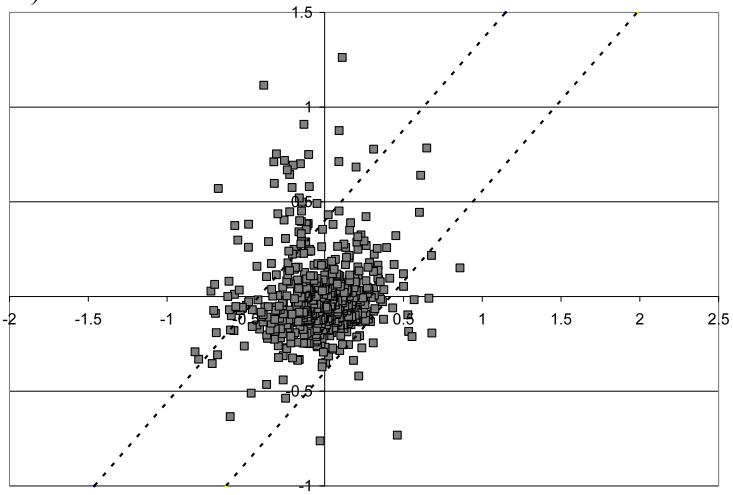

Figure 2

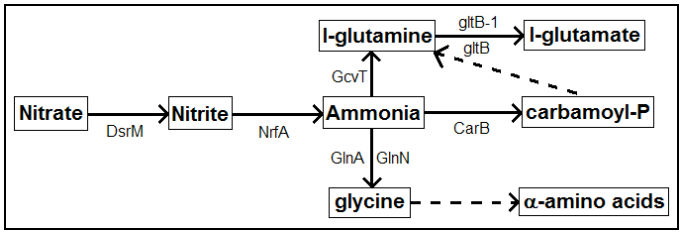
l-glutamine
gltB-1
l-glutamate
gltB
GcvT
Nitrate
DsrM
Nitrite
NrfA
Ammonia
CarB
carbamoyl-P
GlnA
GlnN
glycine
α-amino acids

Table 1- Observed proteins in the nitrate reduction pathway. The average $\log_2$ ratio of nitrate stressed (tag_{116} and tag_{117}) to control (tag_{115}) sample are shown. Proteins are considered to be significantly changing above or below 0.4.

DVU[16]	Gene Name	Description	Ave Run 1 (±0.12)[a]	Ave Run 2 (±0.20)[a]
DVU0625	nrfA	cytochrome c nitrite reductase, catalytic subunit	0.43	0.52
DVU2064	fabK	oxidoreductase, 2-nitropropane dioxygenase family	-0.73	-0.79
DVU1258	glnN	glutamine synthetase, type III	-0.04	0.01
DVU3392	glnA	glutamine synthetase, type I	0.12	0.05
DVU1684	gcvT	glycine cleavage system T protein	1.22	0.43
DVU0162	carB	carbamoyl-phosphate synthase, large subunit	0.32	0.27
DVU1821	gltB	conserved hypothetical protein	-0.17	-0.11
DVU1823	gltB-1	glutamate synthase, iron-sulfur cluster-binding subunit	-	-0.18
DVU2064	fabK	oxidoreductase, 2-nitropropane dioxygenase family	-0.73	-0.79

a) Internal error is appropriate for entire column, see materials and methods for further details.

Table 2- Predicted regulons in *Dv*H. The average $\log_2$ ratio of nitrate stressed (tag_{116} and tag_{117}) to control (tag_{115}) sample are shown. Proteins are considered to be significantly changing above or below 0.4.

DVU[16]	Gene Name	Description	Ave Run 1 (±0.12)[a]	Ave Run 2 (±0.20)[a]
PerR Regulon				
DVU2318	rbr2	rubrerythrin	0.64	1.38
DVU3095	PerR	peroxide-responsive regulator PerR	-	-
DVU3094	rbr	rubrerythrin	0.08	0.00
DVU3093	rdl	rubredoxin-like protein	-	-
DVU2247	ahpC	alkyl hydroperoxide reductase C	-0.25	-0.30
DVU0772	-	hypothetical protein	-	-
HcpR Regulon				
DVU2956	flrA	sigma-54 dependent transcriptional regulator	-	-
DVU1295	sat	sulfate adenylyltransferase	-0.16	-0.18
DVU0846	ApsB	adenylylsulphate reductase, beta subunit	0.07	0.04
DVU0847	ApsA	adenylyl-sulphate reductase, alpha subunit	-0.01	-0.12
DVU0173	phsA	thiosulfate reductase	-0.01	0.26
DVU0172	phsB	thiosulfate reductase	-0.74	0.12
DVU2286	-	hydrogenase, CooM subunit	0.02	0.43
DVU2287	-	hydrogenase, CooK subunit, selenocysteine-containing	-	-
DVU2288	-	hydrogenase, CooL subunit	0.19	-
DVU2289	b2488	hydrogenase, CooX subunit	0.19	0.32
DVU2290	-	hydrogenase, CooU subunit	0.12	0.44
DVU2291	-	carbon monoxide-induced hydrogenase CooH	-0.09	0.12
DVU2292	hypA	hydrogenase nickel insertion protein HypA	-	-
DVU2293	cooF	iron-sulfur protein CooF	-0.27	-
DVU3215	drrA	response regulator	-	-
DVU3216	cckA	sensor histidine kinase	-	-
DVU1080	-	iron-sulfur cluster-binding protein	-	-
DVU1081	-	iron-sulfur cluster-binding protein	-	-
DVU0186	-	conserved hypothetical protein	0.14	-0.12
DVU2543	b0873	hybrid cluster protein	0.32	0.38
DVU2544	-	iron-sulfur cluster-binding protein	-0.16	0.24
DVU2545	-	alcohol dehydrogenase, iron-containing	-	0.01
DVU2546	-	sensory box histidine kinase	-	-

a) Internal error is appropriate for entire column, see materials and methods for further details.

Table 3- Selected high confidence proteins, categorized by function. The average $\log_2$ ratio of nitrate stressed (tag_{116} and tag_{117}) to control (tag_{115}) sample are shown. Proteins are considered to be significantly changing above or below 0.4. ABC transporters form the most represented class of upregulated proteins.

DVU[16]	Gene Name	Description	Ave Run 1 (±0.12)[a]	Ave Run 2 (±0.20)[a]
Thioredoxin				
DVU0283	-	AhpF family protein/thioredoxin reductase	-0.27	-0.34
DVU1457	trxB	thioredoxin reductase	-0.31	-1.05
DVU2247	ahpC	alkyl hydroperoxide reductase C	-0.25	-0.30
DVU3212	nox	pyridine nucleotide-disulfide oxidoreductase	-0.21	-0.23
DVU3379	-	ribonucleoside-diphosphate reductase	0.24	0.27
Oxidative Stress Genes				
DVU0019	ngr	nigerythrin	0.36	0.57
DVU1228	tpX	thiol peroxidase	0.43	0.51
DVU2318	rbr2	rubrerythrin, putative	0.64	1.38
DVU2410	sodB	superoxide dismutase, Fe	0.58	0.57
DVU3183	rbO	desulfoferrodoxin	0.82	1.12
Chemotaxis Proteins				
DVU0170	-	methyl-accepting chemotaxis protein	0.19	1.03
DVU0591	mcpD	methyl-accepting chemotaxis protein	0.28	0.77
DVU1857	-	methyl-accepting chemotaxis protein	0.77	0.55
DVU1904	cheW-2	chemotaxis protein CheW	0.18	0.25
DVU2078	cheB-2	protein-glutamate methylesterase CheB	0.51	0.86
DVU2309	-	methyl-accepting chemotaxis protein	0.39	0.41
DVU2444	flaB3	flagellin	-0.35	-0.31
DVU3035	-	methyl-accepting chemotaxis protein	0.57	0.93
Glutamate to Glutamine				
DVU0161	purF	amidophosphoribosyltransferase	-0.35	-0.34
DVU1953	proA	gamma-glutamyl phosphate reductase	-0.39	-0.42
Response Regulators				
DVU0138	-	response regulator	0.54	1.46
DVU0259	divK	DNA-binding response regulator	0.34	0.71
DVU2966	-	response regulator	0.66	1.43
DVU3023	atoC	sigma-54 dependent DNA-binding response regulator	0.25	0.39
Cytochrome				
DVU1817	cyf	cytochrome c-553	0.51	0.57
DVU1890	hemC	porphobilinogen deaminase	0.76	0.82
DVU2483	-	cytochrome c family protein	0.40	0.69
Selected Conserved Hypotheticals				
DVU0595	-	conserved hypothetical protein	1.06	1.48
DVU0884	ftrB	conserved hypothetical protein	0.86	1.59
DVU2138	-	conserved hypothetical protein	-0.51	-0.61
DVU3118	-	conserved hypothetical protein	1.06	1.57
ABC Transporters Upregulated				
DVU0107	glnH	glutamine ABC transporter, periplasmic glutamine-binding protein	1.10	1.24
DVU0386	glnH	amino acid ABC transporter, periplasmic amino acid-binding protein	0.89	2.09
DVU0547	-	high-affinity branched chain amino acid ABC transporter, periplasmic	0.80	0.87
DVU0712	-	amino acid ABC transporter, periplasmic-binding protein	0.87	0.74
DVU0745	-	ABC transporter, periplasmic substrate-binding protein	1.51	0.76
DVU0752	-	amino acid ABC transporter, amino acid-binding protein	0.23	0.40
DVU0968	-	amino acid ABC transporter, ATP-binding protein	0.38	0.47
DVU1017	rtxB	ABC transporter, ATP-binding protein/permease protein	0.53	0.31
DVU1238	-	amino acid ABC transporter, periplasmic amino acid-binding protein	0.71	0.77
DVU1343	znuA	periplasmic component of zinc ABC transporter	0.37	0.64
DVU1937	-	phosphonate ABC transporter, periplasmic phosphonate-binding protein	0.95	0.74
DVU2297	-	glycine/betaine/L-proline ABC transporter, periplasmic-binding protein	0.68	0.95
DVU3162	-	ABC transporter, periplasmic substrate-binding protein	0.61	0.71

a) Internal error is appropriate for entire column, see materials and methods for further details.

Table 4- Sulfate reduction pathway and ATP synthase operon. The average $\log_2$ ratio of nitrate stressed (tag_{116} and tag_{117}) to control (tag_{115}) sample are shown. Proteins are considered to be significantly changing above or below 0.4.

DVU[16]	Gene Name	Description	Ave Run 1 (±0.12)[a]	Ave Run 2 (±0.20)[a]
Sulfate Reduction Pathway				
DVU1295	sat	sulfate adenylyltransferase	-0.16	-0.18
DVU0846	ApsB	adenylylsulphate reductase, beta subunit	0.07	0.04
DVU0847	ApsA	adenylylsulphate reductase, alpha subunit	-0.01	-0.12
DVU0848	QmoA	Quinone-interacting membrane-bound oxidoreductase	0.02	-0.02
DVU0849	QmoB	Quinone-interacting membrane-bound oxidoreductase	0.19	0.19
DVU0850	QmoC	Quinone-interacting membrane-bound oxidoreductase	0.16	0.27
DVU0402	dsrA	dissimilatory sulfite reductase, alpha subunit	0.01	-0.15
DVU0403	dsrB	dissimilatory sulfite reductase, beta subunit	0.02	-0.19
DVU2776	dsrC	dissimilatory sulfite reductase, gamma subunit	0.40	0.33
DVU0404	dsrD	dissimilatory sulfite reductase D	0.50	0.69
DVU1597	sir	sulfite reductase, assimilatory-type	0.45	0.47
DVU1287	DsrO	Periplasmic (Tat), binds 2[4Fe-4S]	-0.13	0.30
DVU1289	DsrK	Cytoplasmic, binds 2 [4Fe-4S]	-0.05	-0.05
ATP Synthase				
DVU0774	atpC	ATP synthase, F1 epsilon subunit	0.14	0.59
DVU0775	atpD	ATP synthase, F1 beta subunit	0.05	0.01
DVU0776	atpG	ATP synthase, F1 gamma subunit	0.13	0.15
DVU0777	atpA	ATP synthase, F1 alpha subunit	-0.12	-0.10
DVU0778	atpH	ATP synthase, F1 delta subunit	0.02	0.29
DVU0779	atpF2	ATP synthase F0, B subunit	0.46	0.15
DVU0780	atpF1	ATP synthase F0, B subunit	-0.01	0.36

a) Internal error is appropriate for entire column, see materials and methods for further details.